Experimental and Molecular Pathology 143 (2025) 104973

Contents lists available at ScienceDirect

Experimental and Molecular Pathology

journal homepage: www.elsevier.com/locate/yexmp

From asbestos exposure to carcinogenesis: Transcriptomic signatures in malignant pleural mesothelioma

Diletta Rosati [a,b], Bianca Giulia Maurizi [a,b], Viola Bianca Serio [a,b], Debora Maffeo [a,b], Angela Rina [b,c], Francesca Mari [b,c], Maria Palmieri [a,b], Antonio Giordano [b,d], Elisa Frullanti [a,b,*]

[a] Cancer Genomics & Systems Biology Laboratory, University of Siena, 53100 Siena, Italy
[b] Med Biotech Hub and Competence Centre, Department of Medical Biotechnologies, University of Siena, 53100 Siena, Italy
[c] UOC Laboratorio di Assistenza e Ricerca Traslazionale, Azienda Ospedaliero-Universitaria Senese, Siena, Italy
[d] Sbarro Institute for Cancer Research and Molecular Medicine, Center for Biotechnology, Department of Biology, College of Science and Technology, Temple University, Philadelphia, PA 19122, USA

ARTICLE INFO

Keywords:
Malignant pleural mesothelioma (MPM)
Asbestos exposure
Differentially expressed genes (DEGs)
Oxidative stress
Biomarkers

ABSTRACT

Background: The incidence of malignant pleural mesothelioma (MPM) has surged due to widespread asbestos exposure, particularly since the mid-20th century. Despite significant advancements in cancer treatment, an effective cure for MPM remains elusive, largely due to a limited understanding of the molecular mechanisms underlying asbestos-related carcinogenesis. This exploratory study aims to uncover gene expression patterns uniquely altered in mesothelioma patients with documented asbestos exposure, providing a solid foundation for future research focused on identifying novel prognostic and predictive biomarkers.

Methods: Publicly available RNA sequencing data were analyzed through a bioinformatics pipeline to perform differential gene expression analysis. Additionally, functional enrichment analysis was applied to highlight significantly enriched Gene Ontology (GO) terms related to biological processes, molecular functions, and cellular components, offering insights into the molecular pathways involved in MPM development.

Results: The analysis uncovered a set of differentially expressed genes (DEGs) in MPM patients with documented asbestos exposure, as well as key GO terms. These enriched biological terms reflect processes such as ion homeostasis and oxidative stress response, providing crucial information on the cellular alterations driven by asbestos exposure.

Conclusion: This study's findings deepen our understanding of the molecular landscape underlying asbestos-induced carcinogenesis in MPM. The identification of specific DEGs and enriched GO terms lays the foundation for future investigations, including the development of biomarkers, with potential implications for the diagnostic and prognostic assessment of MPM.

1. Introduction

Malignant pleural mesothelioma (MPM) is a rare and highly aggressive cancer primarily linked to asbestos exposure. Despite advancements in research, the prognosis for patients with MPM remains poor, with a median survival of up to 18 months (Baas et al., 2015). Common symptoms include chest pain, difficulty breathing, fatigue, coughing, loss of appetite, and sleep disturbances (Moore et al., 2009). Asbestos exposure was recognized as the primary cause of MPM over 60 years ago (Wagner et al., 1960), and the dose-dependent relationship between asbestos and MPM is now widely accepted (Noonan, 2017). The World Health Organization (WHO) estimates that asbestos-related diseases cause approximately 92,250 deaths worldwide each year, with occupational exposure accounting for over 80 % of cases (Baas et al.,

Abbreviations: MPM, Malignant Pleural Mesothelioma; DEGs, Differentially Expressed Genes; DGE, Differential Gene Expression; GO, Gene Ontology; ROS, Reactive Oxygen Species; PCA, Principal Component Analysis; PA, Parallel Analysis; FDR, False Discovery Rate; TCGA, The Cancer Genome Atlas; MESO, Mesothelioma project dataset; IARC, International Agency for Research on Cancer; WHO, World Health Organization; MA plot, Mean-Average Plot; ANOVA, Analysis of Variance; DAVID, Database for Annotation, Visualization, and Integrated Discovery; UMAP, Uniform Manifold Approximation and Projection; CV, Coefficient of Variation; l2FC, Log2 Fold Change; BP, Biological Processes; CC, Cellular Components; MF, Molecular Functions.

* Corresponding author at: Cancer Genomics & Systems Biology Laboratory, University of Siena, Via A. Moro 2, 53100 Siena, Italy.
E-mail address: elisa.frullanti@dbm.unisi.it (E. Frullanti).

https://doi.org/10.1016/j.yexmp.2025.104973
Received 3 April 2025; Received in revised form 14 May 2025; Accepted 16 May 2025
Available online 20 May 2025

2015). Although many countries have banned asbestos, its environmental persistence and continued production in some nations maintain high global health risks (Brims, 2021).

Asbestos, classified as a Group 1 carcinogen by the International Agency for Research on Cancer (IARC), is one of the primary occupational carcinogens linked to MPM (Ospina et al., 2019). Exposure occurs mainly through inhalation of fibers. High-risk occupations include construction and shipbuilding, but domestic and environmental exposure also contribute (Vimercati et al., 2019). Asbestos fibers, particularly amphibole types, are more persistent and dangerous than chrysotile fibers, with a greater risk associated with fibers longer than 10–20 μm (Barlow et al., 2017). Inhalation of fibers causes chronic inflammation, driven by interactions between mesothelial cells and macrophages, releasing cytokines and reactive oxygen species (ROS), which perpetuate cellular damage (Zolondick et al., 2021). Recent studies suggest that ferroptosis, an iron-dependent form of cell death, may play a role in MPM progression (Ito et al., 2020) (Ito et al., 2021).

Genetic mutations play a crucial role in the pathogenesis of MPM, with frequent alterations in tumor suppressor genes such as BAP1, CDKN2A, and NF2 (Cheung et al., 2017). Sequencing studies have also identified additional mutations in genes like TP53 and SETD2, contributing to tumor development (Bueno et al., 2016). Genetic predisposition is significant, with germline mutations in BAP1 increasing the risk of mesothelioma in individuals with a history of asbestos exposure (Betti et al., 2017). In this context, biomarkers offer a promising avenue for improving early diagnosis and prognosis in MPM, reducing the need for invasive techniques and providing valuable insights into treatment efficacy. Biomarkers such as serum mesothelin, HMGB1, and fibulin-3 have shown potential for diagnostic use, although no test has yet been clinically validated (Schillebeeckx et al., 2021).

This study aims to identify gene expression profiles specific to mesothelioma patients with a history of asbestos exposure. Understanding the mechanisms of asbestos-induced carcinogenesis could provide the basis for the discovery of novel prognostic and predictive biomarkers, with potential implications for improving diagnosis and defining personalized approaches to be explored in future studies on MPM.

2. Materials and methods

2.1. Data extraction and cohort selection

RNA-seq data from patients with MPM were retrieved from the MESO project of The Cancer Genome Atlas (TCGA), accessed in June 2023. In this dataset, asbestos exposure history was positive in 62 %, negative in 18 %, and unavailable or unknown in the rest (Hmeljak et al., 2018). The data were downloaded using the R package TCGAbiolinks, which facilitated access and retrieval of the required information from the TCGA database. Only samples from patients with documented asbestos exposure were included. Initial analyses were non-significant, likely due to imbalance in sample numbers between exposed and unexposed groups, reducing statistical power. To address this, the cohort was adjusted to balance the number of exposed and unexposed samples, while ensuring similar clinical characteristics in both groups. This refinement enhanced statistical robustness and improved the reliability of subsequent analyses.

2.2. Differential gene expression analysis

Differential gene expression (DGE) analysis was conducted using the DESeq2 package in R, applying a negative binomial distribution to estimate fold changes and dispersion (Love et al., 2014). Genes with a mean count below 2 were excluded to improve accuracy (Law et al., 2016). Differentially expressed genes (DEGs) were identified using a log2 fold change ($l2FC > 1$ or $l2FC < -1$) and an FDR-adjusted p-value <0.05. MA and volcano plots were generated to visualize DGE results.

2.3. Statistical and principal component analysis

Statistical comparisons between asbestos-exposed and unexposed groups were made using Welch t-tests to account for unequal variances. ANOVA (Analysis of Variance), followed by Tukey post-hoc tests, was used for multi-group comparisons. Principal component analysis (PCA) was performed on variance-stabilized and scaled data to explore sample clustering. The optimal number of components was determined using parallel analysis (Hayton et al., 2004). Uniform Manifold Approximation and Projection (UMAP) (R package umap v0.2.10.0) was applied to variance-stabilized data to further explore sample stratification. A post hoc power analysis was conducted using RNASeqPower (v1.48.0), based on the sample size (13 vs 12), a significance level (α) of 0.05, dispersion estimates from DESeq2, and a coefficient of variation (CV) of 0.5 (Hart et al., 2013). Power was evaluated across a range of log2 fold changes to assess the ability to detect expression differences given the dataset's variability.

2.4. Functional enrichment analysis

Functional enrichment analysis was carried out using input gene lists consisting of DEGs that resulted as up- and down-regulated in asbestos exposed patients. Gene Ontology (GO) enrichment analysis was performed on DEGs using ClusterProfiler R package, gProfiler, and DAVID tools to identify enriched molecular functions, cellular components, and biological processes. Significance was evaluated using FDR-adjusted p-values (Aleksander et al., 2023). Genes of interest were further identified through literature searches and their association with asbestos exposure using the Comparative Toxicogenomics Database (Davis et al., 2023).

3. Results

The TGCA-MESO dataset provided asbestos exposure data for 59 samples (***Supplementary Table 1***), with 46 samples classified as exposed and 13 as unexposed. Initial DGE analysis with the Welch t-test yielded a non-significant p-value (0.12399), indicating no significant differences between the groups and compromising the study's statistical robustness. To improve the analysis, sample sizes were balanced between exposed and unexposed groups, ensuring homogeneity in clinical characteristics. Given that all samples were tumors and the gene expression differences related to asbestos exposure were likely subtle, only MPM samples with biphasic or epithelioid histology were included. The final dataset selected for analysis consisted of 25 samples, with 13 from asbestos-exposed patients and 12 from unexposed patients. The cohort, detailed in ***Supplementary Table 2*** and ***Supplementary Fig. 1***, includes annotations for exposure group, age, sex, stage, and diagnosis.

To better understand the sensitivity of the analysis given the selected sample size, a post hoc power evaluation was performed. Power analysis (Fig. 1) indicated that the 80 % threshold was reached for genes with large expression differences ($log2FC \geq 1.8$), while the detection of moderately deregulated genes was potentially limited by reduced statistical power. To verify whether measurable transcriptomic differences existed between asbestos-exposed and unexposed patients, a Welch t-test was conducted, yielding a statistically significant result (t-value = 2.2962; p-value = 0.02167). This finding suggested that global gene expression differences between the two groups were unlikely to have occurred by chance, supporting the rationale for conducting a differential gene expression (DGE) analysis. An ANOVA test was also conducted, revealing a significant difference between the two groups (F-value = 6.945; p-value <2e-16). Following the ANOVA, a Tukey post-hoc test was performed, identifying samples with significant differences (***Supplementary Table 3***).

The principal component analysis (PCA) results were visualized in a scree plot (Fig. 2a), showing the variance explained by each of the 25 principal components (PCs). The first principal component (PC1)

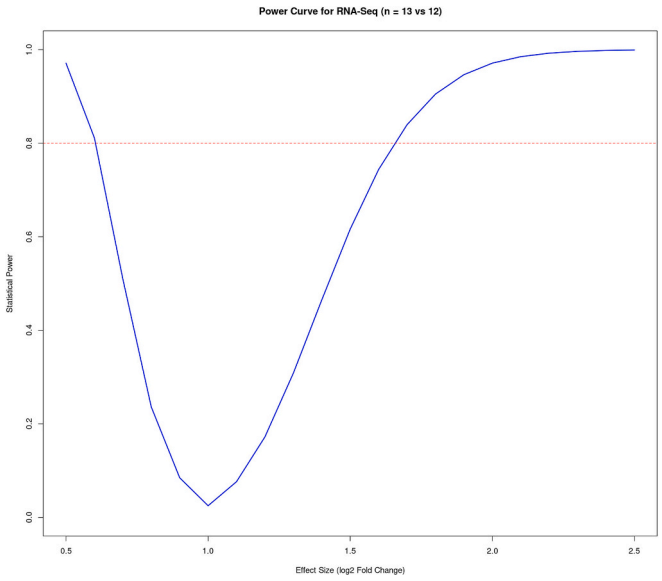

Fig. 1. Post-hoc power analysis for RNA-Seq differential expression analysis comparing asbestos-exposed (n = 13) and unexposed (n = 12) MPM patients. The curve shows statistical power as a function of effect size (log_2 fold change), based on a coefficient of variation (CV) of 0.5 and a significance level of $\alpha = 0.05$. The red dashed line indicates the commonly used 80 % power threshold. The plot illustrates that the analysis is sufficiently powered to detect genes with large expression differences ($log_2FC \geq 1.8$), while the power decreases substantially for smaller effect sizes. (For interpretation of the references to colour in this figure legend, the reader is referred to the web version of this article.)

explained 12.1 % of the variance, with the explained variance decreasing across subsequent components, until PC25, which explained 0 %. A parallel analysis (PA) was performed to determine how many principal components should be retained (Fig. 2b). Based on the PA, it was established that four principal components should be retained. These four components - PC1 (12.1 %), PC2 (10.3 %), PC3 (8.4 %), and PC4 (8 %) - together explained 38.8 % of the total variance. The most effective visual separation between the asbestos-exposed and unexposed groups was observed in the scatter plots for PC1-PC2 and PC1-PC3 (Fig. 2c). Given the limited separation observed with PCA, we applied UMAP as an alternative dimensionality reduction technique. The resulting UMAP plot (Fig. 3) showed a mild distributional tendency between asbestos-exposed and unexposed samples, with some degree of partial grouping. Although the distinction was not sharp and sample overlap was substantial, the observed pattern may suggest the presence of subtle transcriptomic differences associated with asbestos exposure.

As outlined in the methods, the interpretation of DGE analysis relied on key parameters such as log2 fold change ($l2FC > 1$ or $l2FC < -1$), *p*-values, and FDR-adjusted p-values (<0.05) to assess the statistical significance of differentially expressed genes. In accordance with these criteria, 25 genes were identified as up-regulated (***Supplementary Table 4***), and 80 genes were identified as down-regulated (***Supplementary Table 5***) in asbestos-exposed patients. The DGE results were visualized using an MA plot (Fig. 4a), which compares fold change to normalized mean counts. Genes above the red line represent those up-regulated in the exposed group, while those below the line are down-regulated. A volcano plot (Fig. 4b) was also generated using the R/Bioconductor package EnhancedVolcano. This plot allowed for easy identification of genes with large fold changes and statistically significant *p*-values. Genes on the right side of the plot are up-regulated, while those on the left side are down-regulated in exposed patients. In summary, the analysis identified 25 genes (0.088 % of the total) that were

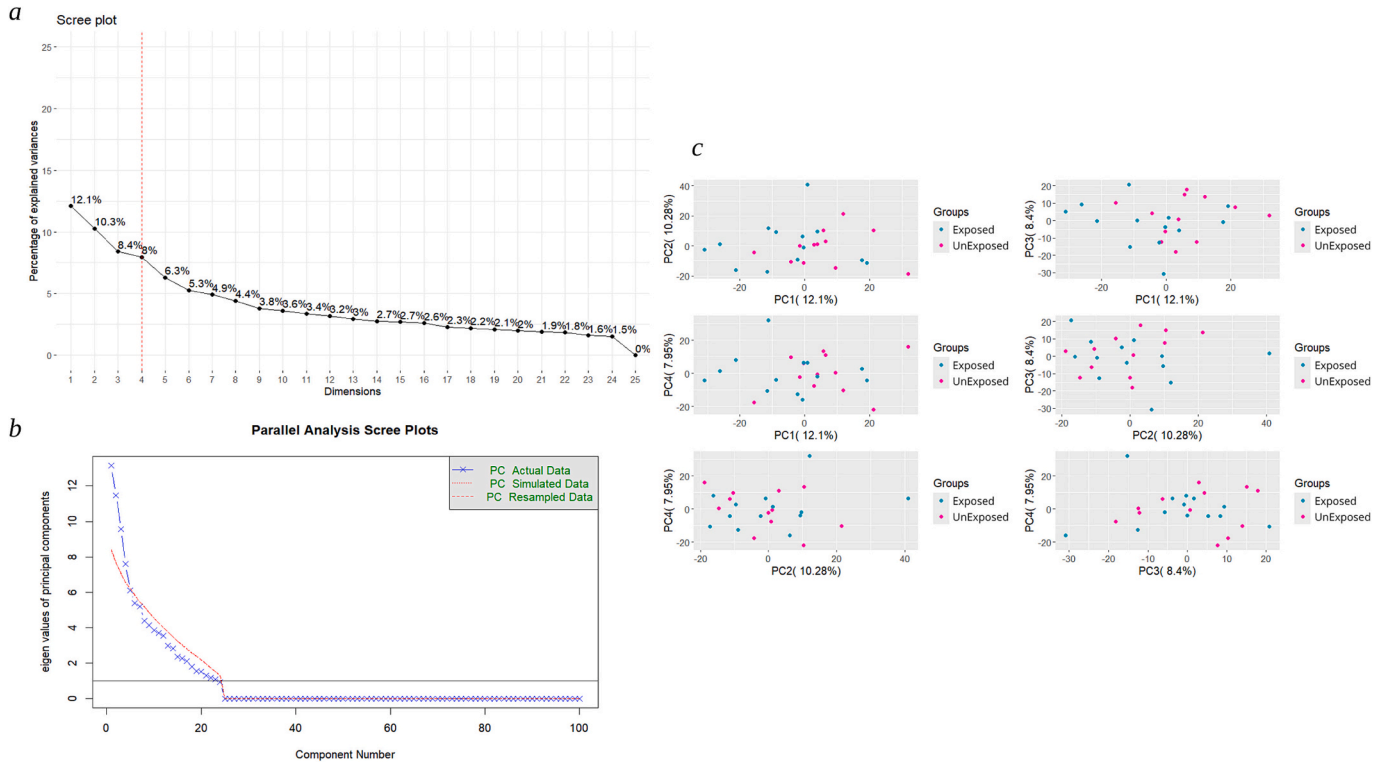

Fig. 2. Parallel Analysis plot & PCA. (a) Scree plot showing the variance explained by each principal component. The Y-axis represents variance, and the X-axis shows the components, helping determine how many to retain. (b) Parallel Analysis plot, with eigenvalues on the Y-axis and the number of factors on the X-axis. The blue line represents the real data's components, intersecting the curve from the simulated dataset. (c) PCA scatter plots illustrating all pairwise combinations between PC1, PC2, PC3, and PC4. Each dot represents a patient, with aquamarine indicating unexposed patients and pink representing asbestos-exposed patients. (For interpretation of the references to colour in this figure legend, the reader is referred to the web version of this article.)

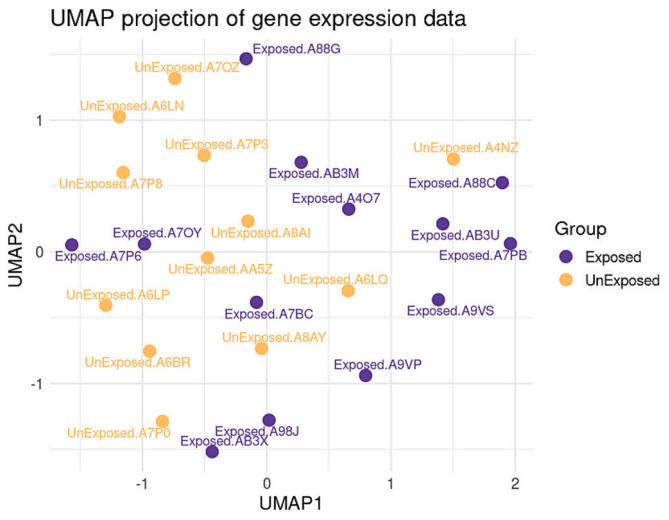

Fig. 3. Uniform Manifold Approximation and Projection Plot. UMAP projection of variance-stabilized gene expression data from asbestos-exposed (purple) and unexposed (orange) MPM samples. Each point represents an individual sample, labeled with its group and identifier. (For interpretation of the references to colour in this figure legend, the reader is referred to the web version of this article.)

up-regulated and 80 genes (0.28 % of the total) that were down-regulated in asbestos-exposed patients.

The functional enrichment analysis, using the GO annotation database, was performed with three different tools, each presenting the results in distinct formats. The clusterProfiler results were visualized in the dot plots (Fig. 5a *and* Fig. 5b). For the up-regulated DEGs, the top 10 enriched GO terms were primarily related to biological processes (BP), including responses to inorganic substances (GO:0010035), cellular responses to metal ions (GO:0071248), cellular responses to inorganic substances (GO:0071241), and cellular responses to copper ions (GO:0071280). Other significant processes involved copper detoxification (GO:0010273), regulation of hydrogen peroxide metabolism (GO:0010310), and stress responses to metal ions (GO:0097501).

For down-regulated DEGs, the top 10 enriched GO terms included five cellular components (CC), such as the external side of the plasma membrane (GO:0009897), collagen-containing extracellular matrix (GO:0062023), and the endoplasmic reticulum lumen (GO:0005788). Additionally, the analysis highlighted BP relevant to vascular function, including vascular regulation (GO:0003018), angiogenesis regulation (GO:0045765), and vascular permeability control (GO:0043114), as well as glomerulus development (GO:0032835). Heatmaps were generated using clusterProfiler to display the relationships between DEGs and their associated GO terms. Fig. 6a illustrates these correlations for the up-regulated genes, while Fig. 6b focuses on the down-regulated genes in patients with asbestos exposure.

The GO functional enrichment analysis was also visualized using gProfiler. This tool provided detailed tables displaying the enriched GO terms, their FDR-adjusted *p*-values, and the genes associated with each process. The terms shown in the figure represent the key driver terms, identified through a novel filtering algorithm within gProfiler, which refined the list of results. All terms listed in the tables were statistically significant, with FDR-adjusted p-values below 0.05. The complete results for up-regulated DEGs can be accessed at this link: https://biit.cs.ut.ee/gplink/l/m44bc5q8TL, and for down-regulated DEGs at: https://biit

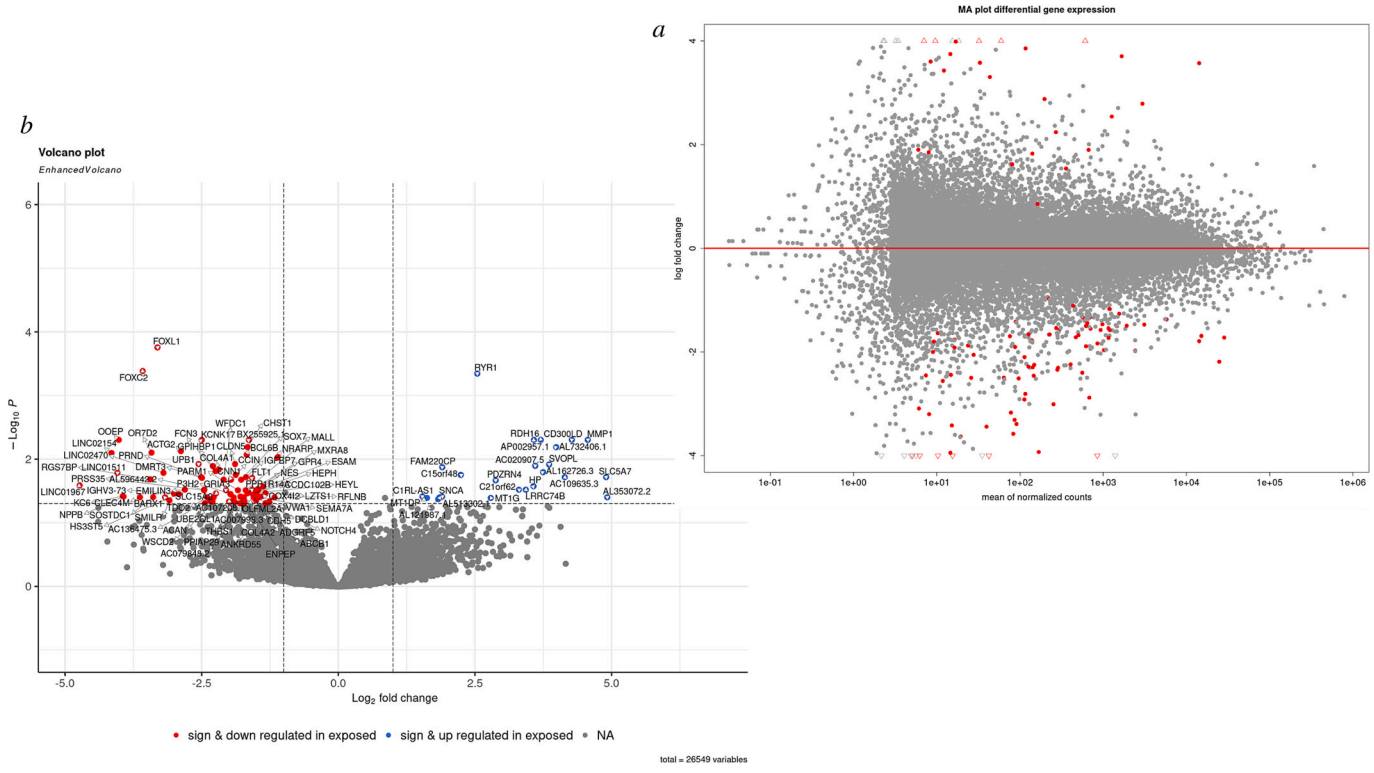

Fig. 4. (a) MA plot. The scatter plot shows mean normalized counts (x-axis) versus log2 fold changes (y-axis) for each gene. Dots above the red line represent up-regulated genes, while those below indicate down-regulated genes in asbestos-exposed patients. Red dots highlight statistically significant differentially expressed genes, with red triangles marking genes with log2 fold changes beyond ±4, outside the plot's scale. (b) Volcano plot. This scatter plot displays *p*-value (y-axis) against log2 fold change (x-axis) for each gene. The horizontal line marks the significance threshold (p-value <0.05), with genes above it considered significant. Vertical lines show log2 fold change cutoffs (l2FC > 1 or l2FC < −1). Blue dots represent significantly upregulated genes in asbestos-exposed patients, while red dots indicate down regulated genes. This pattern reverses for the unexposed group. (For interpretation of the references to colour in this figure legend, the reader is referred to the web version of this article.)

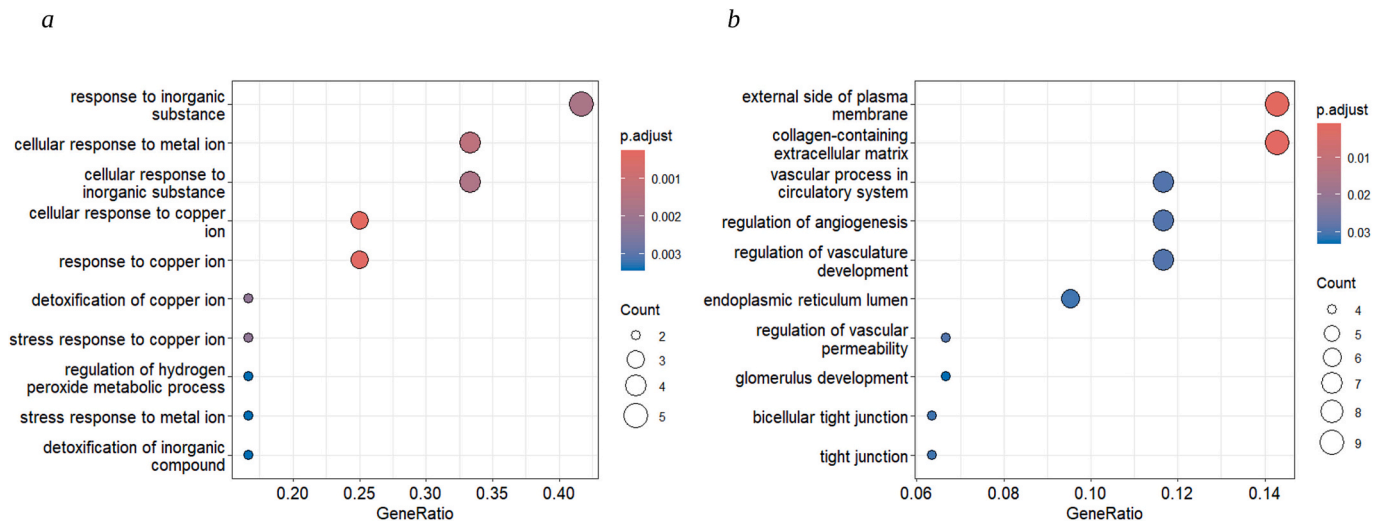

Fig. 5. Functional enrichment analysis with ClusterProfiler. The x-axis shows the GeneRatio, representing the proportion of DEGs linked to each GO term, while the y-axis lists the top 10 enriched GO terms. Each dot reflects a GO term, with its size indicating the number of DEGs (Count) and its colour representing the adjusted p-value (p.adjust). Panel (a) shows the results for up-regulated genes, and panel (b) displays results for down-regulated genes in asbestos-exposed patients.

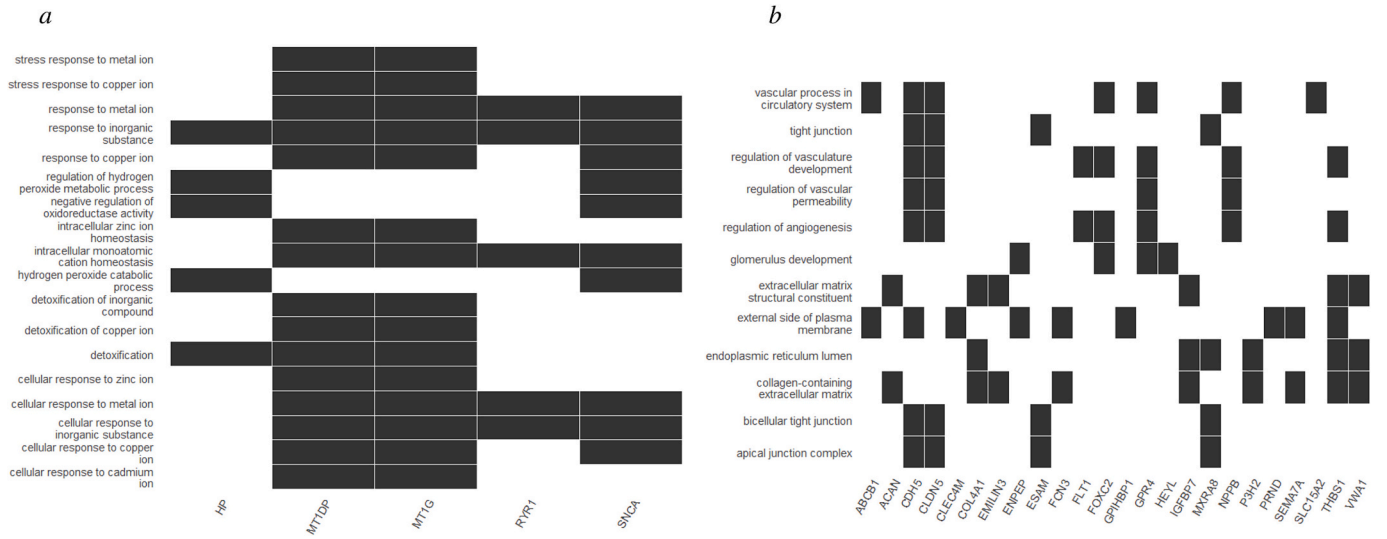

Fig. 6. Enriched GO terms with associated DEGs using ClusterProfiler for (a) up-regulated and (b) down-regulated DEGs in asbestos-exposed patients. Black bars indicate the presence of differentially expressed genes within the enriched Gene Ontology (GO) terms.

.cs.ut.ee/gplink/l/KOPP6wOuRv.

The outcomes of the GO functional enrichment analysis performed with DAVID db were summarized in ***Supplementary Table 6*** *and* ***7***. ***Supplementary Table 6*** highlights the enriched GO terms for up-regulated DEGs, while ***Supplementary Table 7*** covers those for down-regulated DEGs. Only the significantly enriched GO terms are included in the presentation. In terms of the up-regulated genes in patients exposed to asbestos, the BP showing significant enrichment was the cellular response to copper ions (GO:0071280), with genes *MT1G, SNCA, and MT1DP*, and an FDR-adjusted p-value of 0.00895774. For down-regulated genes, the significantly enriched GO terms included collagen-containing extracellular matrix (GO:0062023) with *ACAN, SEMA7A, FCN3, COL4A1, EMILIN3, VWA1, IGFBP7*, and *THBS1*, as well as the external side of the plasma membrane (GO:0009897), involving *CDH5, SEMA7A, FCN3, ENPEP, CLEC4M, THBS1, PRND*, and *GPIHBP1*. Both terms showed statistical significance with an FDR-adjusted p-value of 0.0173. These findings, along with an extensive literature review, helped identify several key genes of interest among the DEGs, which are summarized in ***Supplementary Table 8***.

In order to provide a comprehensive overview of the statistically significant enriched GO terms in the up- and down-regulated genetic profile of asbestos-exposed patients, a Venn diagram (Fig. 7) was constructed. It shows the overlap of results obtained using three enrichment tools: DAVID, ClusterProfiler, and gProfiler. For the up-regulated genes, the only GO term consistently identified by all three tools was the BP "cellular response to copper ion" (GO:0071280), a stress-related response that may reflect altered metal homeostasis in asbestos-exposed tissues. Additional GO terms shared between ClusterProfiler and gProfiler included processes related to oxidative stress regulation (negative regulation of oxidoreductase activity - GO:0051354, detoxification - GO:0098754), ion balance and transport (intracellular monatomic cation homeostasis - GO:0030003, inorganic ion homeostasis - GO:0098771, organic cation transport - GO:0015695), and protein complex formation (protein tetramerization - GO:0051262). These terms collectively suggest an up-regulation of defense mechanisms in response to metal-induced oxidative stress. In the down-regulated profile, the most consistently enriched terms across all tools were the cellular component (CC) "external side of the plasma membrane"

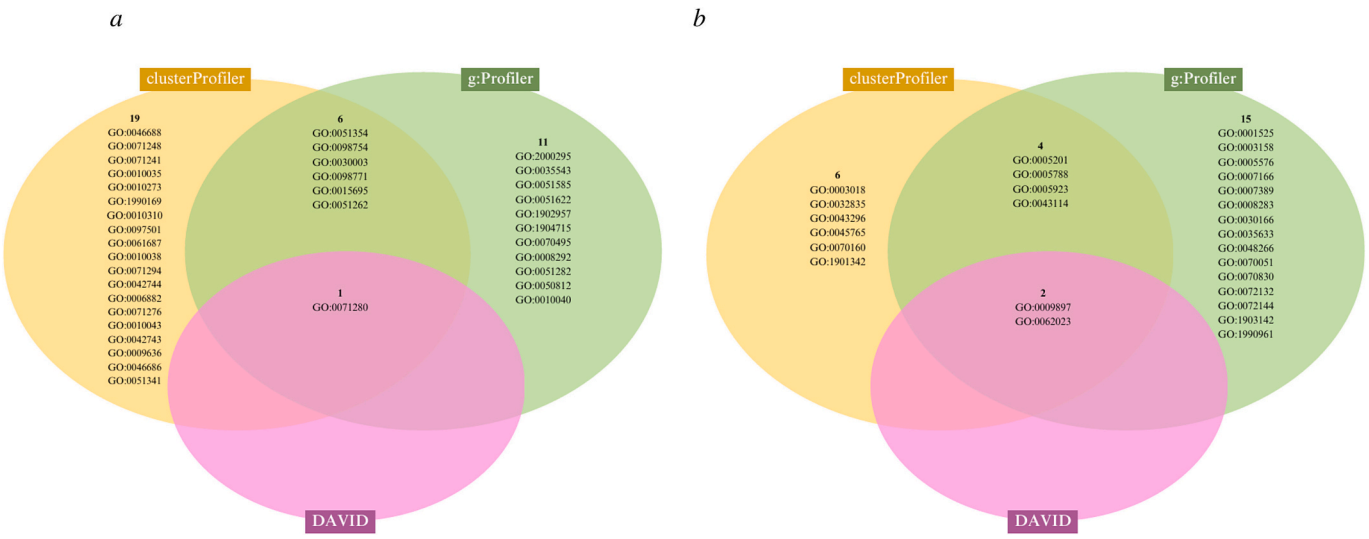

Fig. 7. Venn diagram showing the enriched Gene Ontology (GO) terms identified by ClusterProfiler, g:Profiler, and DAVID. (a) Up-regulated DEGs in asbestos-exposed patients. (b) Down-regulated DEGs in asbestos-exposed patients.

(GO:0009897) and "collagen-containing extracellular matrix" (GO:0062023), highlighting a potential disruption of extracellular matrix organization and cell–cell interactions. ClusterProfiler and gProfiler also shared additional enriched terms, including extracellular matrix structural constituent (GO:0005201) [MF], endoplasmic reticulum lumen (GO:0005788) [CC], bicellular tight junction (GO:0005923) [CC], and the biological process regulation of vascular permeability (GO:0043114). These findings suggest a possible impairment in tissue architecture, cell adhesion, and vascular integrity in asbestos-exposed patients.

4. Discussion

The findings of this study have identified several genes that are differentially expressed in MPM patients with documented asbestos exposure, leading to the characterization of a distinct gene expression profile. While the PCA results did not show well-defined clusters between asbestos-exposed and unexposed groups — an expected outcome given that all samples were from MPM patients — we applied UMAP to the variance-stabilized expression data to further explore potential stratification. Although UMAP did not reveal fully distinct clusters, it showed a mild tendency toward divergence between the groups, with substantial overlap among samples. This subtle pattern is consistent with the statistical results from Welch's *t*-test and ANOVA, which support the presence of modest yet detectable differences between the two groups. Moreover, the post hoc power analysis indicated that the cohort was sufficiently powered to detect genes with substantial expression changes, further supporting the reliability of the identified DEGs.

Functional enrichment analysis using multiple tools revealed distinctive GO terms associated with both the up-regulated and down-regulated genes. The overlap of GO terms, illustrated in the Venn diagram, suggests shared biological mechanisms, including stress response activation and extracellular matrix alterations. These insights support the interpretation of the identified DEGs. Although experimental validation was not feasible, a comprehensive literature review supported the findings and highlighted several key DEGs. For the up-regulated genes, Metallothionein 1D Pseudogene (*MT1DP*) and Metallothionein 1G (*MT1G*) were of particular interest. These genes are likely involved in cellular defense mechanisms against asbestos-induced carcinogenesis, given their roles in metal ion homeostasis, detoxification, and free radical scavenging (Werynska et al., 2015). Increased metallothionein expression in individuals with prolonged asbestos exposure has been reported (Isik et al., 2001), and the upregulation of *MT1G* is also linked to the inhibition of ferroptosis, a process associated with asbestos-induced cancer (Zhang et al., 2022). Metallothionein overexpression is also a recognized marker for tumor progression and drug resistance in a wide range of cancers (Si and Lang, 2018). The haptoglobin gene (*HP*), which resulted also up-regulated, is known for its antioxidant properties. It is mainly expressed in the liver and lungs, and is being studied as a potential biomarker for many diseases, including various forms of malignant neoplasms (Tseng et al., 2004) (Naryzny et al., 2021). HP has previously been reported as differentially expressed in patients with epithelioid MPM (López-Ríos et al., 2006), and its upregulation in asbestos-exposed adipocytes suggests its involvement in asbestos-induced carcinogenesis (Chew et al., 2014). Another significant up-regulated gene in our analysis was the matrix metallopeptidase 1 (*MMP1*) gene encoding a member of the peptidase M10 family of matrix metalloproteinases. Its role in MPM has already been investigated and well-documented (Ying et al., 2020), confirming the validity of our results. *MMP1* expression is known to be influenced by asbestos exposure in both mesothelial and lung epithelial cells (Kroczynska et al., 2006; Perkins et al., 2015a), and these findings are further supported by in vivo studies (Morimoto et al., 1997). It is therefore reasonable to hypothesize that the upregulation of MMP1 observed in our study is directly linked to asbestos exposure.

Our analysis also identified candidates up-regulated in asbestos-exposed patients for which no direct association with asbestos exposure has been reported to date. Synuclein Alpha (*SNCA*) is implicated in cancer and neurodegenerative diseases, and its overexpression has been documented in several malignancies and linked to ferroptosis (Ahmad et al., 2007; Li et al., 2018) (Angelova et al., 2020). However, no direct relationship with asbestos exposure has been established, and its possible involvement in asbestos-related MPM remains an exploratory hypothesis. Similarly, Ryanodine Receptor 1 (*RYR1*), encoding a calcium channel primarily expressed in skeletal muscle (Witherspoon and Meilleur, 2016), was identified among the up-regulated genes. *RYR1* is involved in calcium homeostasis, oxidative stress, and endoplasmic reticulum stress—processes described in the literature as relevant to the biological effects of asbestos (Witherspoon and Meilleur, 2016) (Ryan et al., 2014). Its association with GO terms related to these pathways suggests a potential, although unconfirmed, role in asbestos-related mechanisms.

In the down-regulated gene expression profile, additional genes were identified that may hold considerable biological relevance. Collagen Type IV Alpha 1 Chain (*COL4A1*), a basement membrane component involved in tumor metastasis, is of interest due to its known association

with asbestos (Nymark et al., 2007). Similarly, Insulin-Like Growth Factor Binding Protein 7 (*IGFBP7*) was down-regulated in our study, and previous studies have shown its role in asbestos-exposed cells and potential as a biomarker for lung cancer (Munson et al., 2018; Zhao et al., 2013). Our findings about the down-regulation of the Natriuretic Peptide B gene (*NPPB*) also aligns with those of a previous in vitro study on the DNA methylation profiling of an asbestos-treated MeT5A cell line, suggesting a possible role for *NPPB* in asbestos-related gene regulation (Casalone et al., 2018). Additionally, *NPPB* has been proposed as a marker for NF2-Hippo pathway alterations and/or predict patient prognosis in mesothelioma patients (Sato et al., 2023). Furthermore, the BARX homeobox 1 gene (*BARX1*) and the Forkhead box L1 gene (*FOXL1*), two down-regulated genes in this study, were previously identified as differentially methylated in cells exposed to asbestos (Sato et al., 2023), suggesting their involvement in asbestos-related disease mechanisms. Other down-regulated genes, such as Actin Gamma 2 (*ACTG2*), Solute Carrier Family 15 Member 2 (*SLC15A2*), and Calponin 1 (*CNN1*) genes, have also been linked to asbestos exposure in previous in vitro studies (Munson et al., 2018; Hillegass et al., 2010) (Perkins et al., 2015b). Interestingly, the down-regulation of Olfactory Receptor Family 7 Subfamily D Member 2 (*OR7D2*) contrasts with earlier studies, which reported its up-regulation following asbestos exposure (Nymark et al., 2007). This discordance may arise because Nymark et al. (2007) (Nymark et al., 2007) identified an early response to asbestos exposure (48 h), with ROS release. In contrast, our findings reflect more advanced disease stages, where defense mechanisms against oxidative stress become dominant, and the down-regulation of OR7D2 may indicate an adaptive response to prolonged damage. Similarly, the down-regulation of Thrombospondin 1 (*THBS1*), despite its reported overexpression in MPM tumors (Ohta et al., 1999), suggests a complex role for this gene in asbestos-induced carcinogenesis that warrants further investigation. Finally, Claudin 5 (*CLDN5*) was found to be down-regulated, though previous analyses did not find this gene affected by asbestos (Rouka et al., 2017). Hephaestin (*HEPH*), another down-regulated gene, has been suggested as a potential biomarker for lung cancer (Zacchi et al., 2021) and has been associated with protection against MPM in asbestos-exposed populations (Crovella et al., 2016). Further studies are needed to explore its role in asbestos-induced carcinogenesis. For the remaining DEGs, no available evidence of direct associations with asbestos exposure have currently been reported in the literature, suggesting that additional research is needed to fully understand their potential roles in MPM.

The functional enrichment analysis of the 25 up-regulated genes highlighted several key biological processes, such as inorganic ion homeostasis, regulation of hydrogen peroxide catabolic processes, and detoxification pathways. These findings suggest that asbestos exposure disrupts essential cellular functions, particularly ion regulation and oxidative stress response. Conversely, the analysis of the 80 down-regulated genes revealed significant enrichment in cellular components, specifically the external side of the plasma membrane and the collagen-containing extracellular matrix. This supports the hypothesis that inhaling asbestos fibers could compromise cellular integrity and disrupt cell-matrix interactions.

5. Conclusions and future perspectives

This study identifies a distinct gene expression profile linked to asbestos exposure. The enriched GO terms derived from the functional enrichment analysis offer a foundation for future investigations. In particular, among the up-regulated DEGs, metallothioneins (*MT1DP* and *MT1G*), *SNCA, HP, MMP1*, and *RYR1* stand out. *MT1G* and *MMP1* are well-documented in asbestos-induced carcinogenesis and could act as diagnostic biomarkers for asbestos exposure. In contrast, *SNCA* and *RYR1* have not been previously linked to asbestos exposure. Given their roles in ferroptosis, calcium homeostasis, and oxidative stress, their upregulation requires further investigation. Similarly, the down-regulated DEGs, including *COL4A1, IGFBP7, NPPB, BARX1, FOXL1, ACTG2, OR7D2, SLC15A2, CNN1, THBS1, CLDN5*, and *HEPH*, offer both established and emerging insights. While genes like *IGFBP7* and *COL4A1* have established roles in asbestos-related processes, others, such as *HEPH*, show potential as a biomarker for asbestos-related carcinogenesis, despite limited direct evidence.

Limitations of this study must be acknowledged. One of the primary constraints is the limited sample size, a common challenge in MPM research due to the rarity of the disease. In this study, the cohort size was further adjusted to reduce statistical bias caused by variability within one of the subgroups. Expanding the use of public omics databases and promoting data sharing within the scientific community could help address this first limitation. A larger, more diverse cohort would enable more detailed analyses, accounting for variables such as tumor stage, gender, and age. Although the power analysis confirmed that our study could detect genes with large expression changes, smaller differences may have gone undetected. As a result, moderately deregulated genes—possibly relevant to asbestos-induced carcinogenesis—might be underrepresented. A further limitation is the retrospective classification of asbestos exposure based on TCGA-MESO annotations. Although the TCGA study (Hmeljak et al., 2018) reported asbestos exposure history, it also recommended caution when interpreting exposure-related findings, due to potential limitations in the dataset. To reduce the risk of misclassification, only samples with documented exposure status were included. Nonetheless, a certain degree of uncertainty cannot be excluded and may have contributed to the differences in gene expression between exposed and unexposed groups. Prospective studies with standardized exposure data are needed to validate and extend these findings. Finally, this study lacks experimental validation of the transcriptomic results. In the future, we plan to collaborate with groups conducting lung content analyses and animal studies, with the aim of increasing sample size and variability, and validating our findings. Validation efforts will focus on the genes *MT1G, MMP1, HP*, and *COL4A1*, selected for their involvement in oxidative stress, matrix remodeling, metal ion homeostasis, and extracellular matrix integrity—biological processes relevant to asbestos-related carcinogenesis. Protein-level validation will be performed using Western blotting and immunohistochemistry.

This study serves as a preliminary step toward future research aimed at identifying biomarkers for MPM. Future directions will include both in vitro and in vivo studies, focusing on the functional characterization of the highlighted genes. The ultimate goal is to identify novel diagnostic and prognostic biomarkers, along with candidate molecular targets to be evaluated in future studies, with potential implications in the clinical management of MPM.

Supplementary data to this article can be found online at https://doi.org/10.1016/j.yexmp.2025.104973.

CRediT authorship contribution statement

Diletta Rosati: Writing – original draft, Visualization, Resources, Methodology, Investigation, Formal analysis, Data curation, Conceptualization. **Bianca Giulia Maurizi:** Writing – original draft, Methodology, Formal analysis. **Viola Bianca Serio:** Writing – review & editing, Validation. **Debora Maffeo:** Writing – review & editing. **Angela Rina:** Writing – review & editing. **Francesca Mari:** Writing – review & editing. **Maria Palmieri:** Writing – review & editing, Validation. **Antonio Giordano:** Writing – review & editing, Supervision. **Elisa Frullanti:** Writing – review & editing, Validation, Supervision, Project administration, Funding acquisition, Conceptualization.

Ethics statement

This study is based on publicly available data from The Cancer Genome Atlas (TCGA), which was generated with the approval of institutional review boards at participating institutions, under the

coordination of the National Cancer Institute (NCI) and the National Human Genome Research Institute (NHGRI). No additional ethics approval was required for this secondary analysis of de-identified data.

Funding

This work was supported by the Italian National Institute for Insurance against Accidents at Work (INAIL) within the BRiC-INAIL 2022 call, Piano Attività di Ricerca 2022–2024 (E.F.), under project ID 19: "Identificazione dell'impronta digitale dell'esposizione all'amianto nel mesotelioma."

Declaration of competing interest

The authors declare no conflict of interest.

Acknowledgements

The authors would like to thank the Cancer Genomics & Systems Biology Laboratory at the University of Siena for providing access to the necessary resources for this study, and to the Sbarro Institute for Cancer Research and Molecular Medicine at Temple University for their collaboration and support. The authors also wish to thank the Buzzi Unicem Foundation for awarding this work the Prize for the Best Poster at the 64th Annual Meeting of the Italian Cancer Society – *Science-driven approaches to achieve early diagnosis of cancer and overcome therapy resistance*, held in Milan from September 25-27, 2024.

Data availability

The data analyzed in this study are publicly available through the TCGA-MESO dataset (The Cancer Genome Atlas – Mesothelioma project).

References

Ahmad, M., Attoub, S., Singh, M.N., et al., 2007. γ-Synuclein and the progression of cancer. FASEB J. 21 (13), 3419–3430. https://doi.org/10.1096/fj.07-8379rev.

Aleksander, S.A., Balhoff, J., Carbon, S., et al., 2023. The gene ontology knowledge base in 2023. Genetics 224 (1). https://doi.org/10.1093/genetics/iyad031.

Angelova, P.R., Choi, M.L., Berezhnov, A.V., et al., 2020. Alpha synuclein aggregation drives ferroptosis: an interplay of iron, calcium and lipid peroxidation. Cell Death Differ. 27 (10), 2781–2796. https://doi.org/10.1038/s41418-020-0542-z.

Baas, P., Fennell, D., Kerr, K.M., et al., 2015. Malignant pleural mesothelioma: ESMO clinical practice guidelines for diagnosis, treatment and follow-up. Ann. Oncol. 26 (Suppl. 5). https://doi.org/10.1093/annonc/mdv199.

Barlow, C.A., Grespin, M., Best, E.A., 2017. Asbestos fiber length and its relation to disease risk. Inhal. Toxicol. 29 (12–14), 541–554. https://doi.org/10.1080/08958378.2018.1435756.

Betti, M., Casalone, E., Ferrante, D., et al., 2017. Germline mutations in DNA repair genes predispose asbestos-exposed patients to malignant pleural mesothelioma. Cancer Lett. 405, 38–45. https://doi.org/10.1016/j.canlet.2017.06.028.

Brims, F., 2021. Epidemiology and clinical aspects of malignant pleural mesothelioma. Cancers 13 (16), 4194. https://doi.org/10.3390/cancers13164194.

Bueno, R., Stawiski, E.W., Goldstein, L.D., et al., 2016. Comprehensive genomic analysis of malignant pleural mesothelioma identifies recurrent mutations, gene fusions and splicing alterations. Nat. Genet. 48 (4), 407–416. https://doi.org/10.1038/ng.3520.

Casalone, E., Allione, A., Viberti, C., et al., 2018. DNA methylation profiling of asbestos-treated MeT5A cell line reveals novel pathways implicated in asbestos response. Arch. Toxicol. 92 (5), 1785–1795. https://doi.org/10.1007/s00204-018-2179-y.

Cheung, M., Menges, C.W., Testa, J.R., 2017. Germline and somatic mutations in human mesothelioma and lessons from asbestos-exposed genetically engineered mouse models. In: Asbestos-Related Diseases. IntechOpen. https://doi.org/10.1007/978-3-319-53560-9_8.

Chew, S.H., Okazaki, Y., Nagai, H., et al., 2014. Cancer-promoting role of adipocytes in asbestos-induced mesothelial carcinogenesis through dysregulated adipocytokine production. Carcinogenesis 35 (1), 164–172. https://doi.org/10.1093/carcin/bgt267.

Crovella, S., Bianco, A.M., Vuch, J., et al., 2016. Iron signature in asbestos-induced malignant pleural mesothelioma: a population-based autopsy study. J. Toxicol. Environ. Health A 79 (3), 129–141. https://doi.org/10.1080/15287394.2015.1123452.

Davis, A.P., Wiegers, T.C., Johnson, R.J., et al., 2023. Comparative toxicogenomics database (CTD): update 2023. Nucleic Acids Res. 51 (D1). https://doi.org/10.1093/nar/gkac833.

Hart, S.N., Therneau, T.M., Zhang, Y., Poland, G.A., Kocher, J.P., 2013. Calculating sample size estimates for RNA sequencing data. J. Comput. Biol. 20 (12), 970–978. https://doi.org/10.1089/cmb.2012.0283.

Hayton, J.C., Allen, D.G., Scarpello, V., 2004. Factor retention decisions in exploratory factor analysis: a tutorial on parallel analysis. Organ. Res. Methods 7 (2), 191–205. https://doi.org/10.1177/1094428104263675.

Hillegass, J.M., Shukla, A., MacPherson, M.B., et al., 2010. Mechanisms of oxidative stress and alterations in gene expression by Libby six-mix in human mesothelial cells. Part. Fibre Toxicol. 7, 26. https://doi.org/10.1186/1743-8977-7-26.

Hmeljak, J., Sanchez-Vega, F., Hoadley, K.A., et al., 2018. Integrative molecular characterization of malignant pleural mesothelioma. Cancer Discov. 8 (12), 1548–1565. https://doi.org/10.1158/2159-8290.CD-18-0804.

Isik, R., Metintas, M., Gibbs, A.R., et al., 2001. p53, p21 and metallothionein immunoreactivities in patients with malignant pleural mesothelioma: correlations with the epidemiological features and prognosis of mesotheliomas with environmental asbestos exposure. Respir. Med. 95 (7), 588–593. https://doi.org/10.1053/rmed.2001.1108.

Ito, F., Yanatori, I., Maeda, Y., et al., 2020. Asbestos conceives Fe(II)-dependent mutagenic stromal milieu through ceaseless macrophage ferroptosis and β-catenin induction in mesothelium. Redox Biol. 36, 101616. https://doi.org/10.1016/j.redox.2020.101616.

Ito, F., Kato, K., Yanatori, I., et al., 2021. Ferroptosis-dependent extracellular vesicles from macrophage contribute to asbestos-induced mesothelial carcinogenesis through loading ferritin. Redox Biol. 47, 102174. https://doi.org/10.1016/j.redox.2021.102174.

Kroczynska, B., Cutrone, R., Bocchetta, M., et al., 2006. Crocidolite asbestos and SV40 are cocarcinogens in human mesothelial cells and in causing mesothelioma in hamsters. Proc. Natl. Acad. Sci. USA 103 (38), 14128–14133. https://doi.org/10.1073/pnas.0604544103.

Law, C.W., Alhamdoosh, M., Su, S., et al., 2016. RNA-seq analysis is easy as 1-2-3 with limma, Glimma and edgeR. F1000Res 5, 1408. https://doi.org/10.12688/f1000research.9005.1.

Li, Y., Yu, Z., Jiang, T., et al., 2018. SNCA, a novel biomarker for group 4 medulloblastomas, can inhibit tumor invasion and induce apoptosis. Cancer Sci. 109 (4), 1263–1275. https://doi.org/10.1111/cas.13515.

López-Ríos, F., Chuai, S., Flores, R., et al., 2006. Global gene expression profiling of pleural mesotheliomas: overexpression of Aurora kinases and P16/CDKN2A deletion as prognostic factors and critical evaluation of microarray-based prognostic prediction. Cancer Res. 66 (6), 2970–2979. https://doi.org/10.1158/0008-5472.CAN-05-3907.

Love, M.I., Huber, W., Anders, S., 2014. Moderated estimation of fold change and dispersion for RNA-seq data with DESeq2. Genome Biol. 15 (12), 550. https://doi.org/10.1186/s13059-014-0550-8.

Moore, S., Darlison, L., Tod, A.M., 2009. Living with mesothelioma: a literature review. Eur. J. Cancer Care (Engl) 19 (4), 458–468. https://doi.org/10.1111/j.1365-2354.2009.01170.x.

Morimoto, Y., Tsuda, T., Nakamura, H., et al., 1997. Expression of matrix metalloproteinases, tissue inhibitors of metalloproteinases, and extracellular matrix mRNA following exposure to mineral fibers and cigarette smoke in vivo. Environ. Health Perspect. 105 (Suppl. 5), 1247–1251. https://doi.org/10.1289/ehp.97105s51247.

Munson, P., Lam, Y., Dragon, J., et al., 2018. Exosomes from asbestos-exposed cells modulate gene expression in mesothelial cells. FASEB J. 32 (8), 4328–4342. https://doi.org/10.1096/fj.201701291RR.

Naryzny, S.N., Legina, O.K., et al., 2021. Biochem. (Mosc.) Suppl. B: Biomed. Chem. 15 (3), 184–198. https://doi.org/10.1134/S1990750821030069.

Noonan, C.W., 2017. Environmental asbestos exposure and risk of mesothelioma. Ann. Transl. Med. 5 (11), 234. https://doi.org/10.21037/atm.2017.03.74.

Nymark, P., Lindholm, P.M., Korpela, M.V., et al., 2007. Gene expression profiles in asbestos-exposed epithelial and mesothelial lung cell lines. BMC Genomics 8, 62. https://doi.org/10.1186/1471-2164-8-62.

Ohta, Y., Shridhar, V., Kalemkerian, G.P., et al., 1999. Thrombospondin-1 expression and clinical implications in malignant pleural mesothelioma. Cancer 85 (12), 2570–2576.

Ospina, D., Villegas, V.E., Rodríguez-Leguizamón, G., Rondón-Lagos, M., 2019. Analyzing biological and molecular characteristics and genomic damage induced by exposure to asbestos. Cancer Manag. Res. 11, 4997–5012. https://doi.org/10.2147/CMAR.S205723.

Perkins, T.N., Peeters, P.M., Shukla, A., et al., 2015a. Indications for distinct pathogenic mechanisms of asbestos and silica through gene expression profiling of the response of lung epithelial cells. Hum. Mol. Genet. 24 (5), 1374–1389. https://doi.org/10.1093/hmg/ddu551.

Perkins, T.N., Peeters, P.M., Shukla, A., et al., 2015b. Indications for distinct pathogenic mechanisms of asbestos and silica through gene expression profiling of the response of lung epithelial cells. Hum. Mol. Genet. 24 (5), 1374–1389. https://doi.org/10.1093/hmg/ddu551.

Rouka, E., Vavougios, G.D., Solenov, E.I., et al., 2017. Transcriptomic analysis of the claudin interactome in malignant pleural mesothelioma: evaluation of the effect of disease phenotype, asbestos exposure, and CDKN2A deletion status. Front. Physiol. 8, 156. https://doi.org/10.3389/fphys.2017.00156.

Ryan, A.J., Larson-Casey, J.L., He, C., et al., 2014. Asbestos-induced disruption of calcium homeostasis induces endoplasmic reticulum stress in macrophages. J. Biol. Chem. 289 (48), 33391–33403. https://doi.org/10.1074/jbc.M114.579870.

Sato, T., Akao, K., Sato, A., et al., 2023. Aberrant expression of NPPB through YAP1 and TAZ activation in mesothelioma with hippo pathway gene alterations. Cancer Med. 12(12, 13586–13598. https://doi.org/10.1002/cam4.6056.

Schillebeeckx, E., van Meerbeeck, J.P., Lamote, K., 2021. Clinical utility of diagnostic biomarkers in malignant pleural mesothelioma: a systematic review and meta-analysis. Eur. Respir. Rev. 30 (162), 210057. https://doi.org/10.1183/16000617.0057-2021.

Si, M., Lang, J., 2018. The roles of metallothioneins in carcinogenesis. J. Hematol. Oncol. 11 (1), 107. https://doi.org/10.1186/s13045-018-0645-x.

Tseng, C.F., Lin, C.C., Huang, H.Y., et al., 2004. Antioxidant role of human haptoglobin. Proteomics 4 (8), 2221–2228. https://doi.org/10.1002/pmic.200300787.

Vimercati, L., Cavone, D., Caputi, A., et al., 2019. Malignant mesothelioma in construction workers: the Apulia regional mesothelioma register, southern Italy. BMC. Res. Notes 12 (1), 636. https://doi.org/10.1186/s13104-019-4675-4.

Wagner, J.C., Sleggs, C.A., Marchand, P., 1960. Diffuse pleural mesothelioma and asbestos exposure in the North Western Cape Province. Occup. Environ. Med. 17 (4), 260–271. https://doi.org/10.1136/oem.17.4.260.

Werynska, B., Pula, B., Kobierzycki, C., et al., 2015. Metallothioneins in the lung cancer. Folia Histochem. Cytobiol. 53 (1), 1–10. https://doi.org/10.5603/FHC.a2015.0009.

Witherspoon, J.W., Meilleur, K.G., 2016. Review of RyR1 pathway and associated pathomechanisms. Acta Neuropathol. Commun. 4 (1), 121. https://doi.org/10.1186/s40478-016-0392-6.

Ying, S., Wang, Y., Lyu, L., 2020. Potential roles of matrix metalloproteinases in malignant mesothelioma. In: Asbestos-Related Diseases. IntechOpen. https://doi.org/10.5772/intechopen.88783.

Zacchi, P., Belmonte, B., Mangogna, A., et al., 2021. The ferroxidase hephaestin in lung cancer: pathological significance and prognostic value. Front. Oncol. 11, 638856. https://doi.org/10.3389/fonc.2021.638856.

Zhang, W., Luo, M., Xiong, B., et al., 2022. Upregulation of Metallothionein 1 G (MT1G) negatively regulates ferroptosis in clear cell renal cell carcinoma by reducing glutathione consumption. J. Oncol. 2022, 4000617. https://doi.org/10.1155/2022/4000617.

Zhao, J., Wang, Z., Wang, Z., et al., 2013. Expression and clinical significance of IGF-1, IGFBP-3, and IGFBP-7 in serum and lung cancer tissues from patients with non-small cell lung cancer. Onco. Targets Ther. 6, 1437–1444. https://doi.org/10.2147/OTT.S51997.

Zolondick, A.A., Gaudino, G., Xue, J., et al., 2021. Asbestos-induced chronic inflammation in malignant pleural mesothelioma and related therapeutic approaches—a narrative review. Precis Cancer Med. 4, 27. https://doi.org/10.21037/pcm-21-12.